On modeling sea clutter by noisy chaotic dynamics

Wen-wen Tung[1], Jing Hu[2], Jianbo Gao[2], Robert S. Lynch[3], and Genshe Chen[4]
[1]Department of Earth & Atmospheric Sciences,
Purdue University, West Lafayette, IN 47907
[2]Department of Electrical and Computer Engineering
University of Florida, Gainesville, FL 32611
[3]Signal Processing Branch
Naval Undersea Warfare Center, Newport, RI 02841
[4]DCM Research Resources LLC
Germantown, MD 20874

ABSTRACT

Modeling sea clutter by chaotic dynamics has been an exciting yet heatedly debated topic. To resolve controversies associated with this approach, we use the scale-dependent Lyapunov exponent (SDLE) to study sea clutter. The SDLE has been shown to be able to unambiguously distinguish chaos from noise. Our analyses of almost 400 sea clutter datasets measured by Professor Simon Haykin suggest that on very short time scales, sea clutter may be classified as noisy chaos, characterized by a parameter γ, which characterizes the speed of information loss. It is shown that γ can be used to very effectively detect low observable targets within sea clutter.

1 INTRODUCTION

Understanding the nature of sea clutter is crucial to the successful modeling of sea clutter as well as to facilitate target detection within sea clutter. To this end, an important question to ask is whether sea clutter is stochastic or deterministic. Since the complicated sea clutter signals are functions of complex (sometimes turbulent) wave motions on the sea surface, while wave motions on the sea surface clearly have their own dynamical features that are not readily described by simple statistical features, it is very appealing to understand sea clutter by considering some of their dynamical features. In the past decade, Haykin et al. have carried out analysis of some sea clutter data using chaos theory [1,2], and concluded that sea clutter was generated by an underlying chaotic process. Recently, their conclusion has been challenged by a number of researchers [3–9]. In particular, Unsworth et al. [6, 7] have demonstrated that

Signal Processing, Sensor Fusion, and Target Recognition XVII, edited by Ivan Kadar
Proc. of SPIE Vol. 6968, 69681G, (2008) · 0277-786X/08/$18 · doi: 10.1117/12.777204

the two main invariants used by Haykin et al. [1, 2], namely the "maximum likelihood of the correlation dimension estimate" and the "false nearest neighbors" are problematic in the analysis of measured sea clutter data, since both invariants may interpret stochastic processes as chaos. They have also tried an improved method, which is based on the correlation integral of Grassberger and Procaccia [10] and has been found to be effective in distinguishing stochastic processes from chaos. Still, no evidence of determinism or chaos has been found in sea clutter data.

To reconcile ever growing evidence of stochasticity in sea clutter with their chaos hypothesis, recently, Haykin et al. [11] have suggested that the non-chaotic feature of sea clutter could be due to many types of noise sources in the data. To test this possibility, McDonald and Damini [12] have tried a series of low-pass filters to remove noise; but again they have failed to find any chaotic features. Furthermore, they have found that the commonly used invariant measures of chaos, the correlation dimension and the largest positive Lyapunov exponent, computed by conventional methods, cannot be used to distinguish measured sea clutter data from simulated stochastic processes, and that a nonlinear predictor shows little improvement over linear prediction.

Most of the studies in [3–7] are indirect, because they were conducted by comparing measured sea clutter data with simulated stochastic processes. While they suggest that sea clutter is unlikely to be truly chaotic in a rigorous mathematical sense, they have also generated a number of fundamental questions. For example, we can ask: 1) The wave-turbulence interactions on the sea surface clearly have their distinct dynamics. Can we properly and directly characterize them by going beyond the standard chaos theory and conventional statistical descriptions? 2) Will studies along this line be of any help for target detection within sea clutter?

In this paper, we employ a recently developed multiscale complexity measure, the scale-dependent Lyapunov exponent (SDLE) [13, 14], to study sea clutter. The SDLE has been shown to be able to classify various types of complex motions, including low-dimensional chaos, stochastic oscillations, random $1/f$ processes, random Levy processes, and complex motions with multiple scaling behaviors, and thus is able to unambiguously distinguish chaos from noise. By analyzing almost 400 sea clutter datasets, we show that although sea clutter is not chaotic in terms of standard deterministic chaos theory, on very short time scales, sea clutter may be classified as noisy chaos, characterized by a single parameter γ, characterizing the speed of information loss. We are thus able to reconcile all the researches conducted so far. More interestingly, we show that γ can be used to very effectively detect low observable targets within sea clutter.

The remainder of the paper is organized as follows. In Sec. 2, we describe multiscale analysis by SDLE. In Sec. 3, we first describe sea clutter data, then carry out multiscale analysis of sea clutter and develop effective methods for detecting small targets within sea clutter. In Sec. 4, we make a few concluding remarks.

2 MULTISCALE ANALYSIS BY THE SCALE-DEPENDENT LYAPUNOV EXPONENT (SDLE)

2.1 Definition of the SDLE

The SDLE is defined in a phase space. To set up a proper stage to analyze sea clutter using dynamical systems theory, it is important to first briefly review the concept of phase space. For simplicity, let us consider a system with two state variables, X_1 and X_2. When monitoring the motion of the system in time, one can plot out the waveforms for $X_1(t)$ and $X_2(t)$. Alternatively, one can monitor the trajectory defined by $(X_1(t), X_2(t))$, where the time, t, appears as an implicit parameter. The space spanned by X_1 and X_2 is called the phase space (or state space). The dimension of the phase space is the number of degrees of freedom of the system. When the system is modeled by partial differential equations (PDEs) or stochastic partial (or ordinary) differential equations, the dimension of the phase space is infinite. However, the dimension of the attractor of the dynamics could still be quite low, even if the phase space is infinite-dimensional. For example, a stable fixed point solution has a dimension of zero, while a limit cycle solution has a dimension of one.

In many experimental situations, often only a scalar time series $x(1), x(2), \cdots, x(n)$ is available. In such a situation, a suitable phase space may be obtained by using time delay embedding to construct vectors of the form [14]:

$$V_i = [x(i), x(i+L), ..., x(i+(m-1)L)], \tag{1}$$

where m and L are called the embedding dimension and the delay time, respectively. For chaotic systems, m and L have to be chosen according to certain optimization criterion [14]. For a stochastic process, which is infinite-dimensional, the embedding procedure transforms a self-affine stochastic process to a self-similar process in a phase space. Therefore, specific values of m and L are not important, so long as $m > 1$. For example, one could simply choose $m = 2,\ L = 1$ [13, 14].

To define the SDLE, we consider an ensemble of trajectories in the reconstructed phase space. Let us denote the initial separation between two nearby trajectories by ε_0, and their *average separation* at time t and $t + \Delta t$ by ε_t and $\varepsilon_{t+\Delta t}$, respectively. The SDLE $\lambda(\varepsilon_t)$ is defined through equations [13, 14]

$$\varepsilon_{t+\Delta t} = \varepsilon_t e^{\lambda(\varepsilon_t)\Delta t}, \quad \text{or} \quad \lambda(\varepsilon_t) = \frac{\ln \varepsilon_{t+\Delta t} - \ln \varepsilon_t}{\Delta t}. \tag{2}$$

Equivalently, we have a differential equation for ϵ_t,

$$\frac{d\epsilon_t}{dt} = \lambda(\epsilon_t)\epsilon_t, \quad \text{or} \quad \frac{d\ln\epsilon_t}{dt} = \lambda(\epsilon_t). \tag{3}$$

Given a discrete time series data, the smallest Δt possible is the sampling time τ.

In our recent work [13, 14], we have found a number of distinctive scalings for the SDLE. Those most relevant to sea clutter modeling are summarized below:

(a) For deterministic chaos, for small ϵ, the SDLE equals the largest positive Lyapunov exponent λ_1,

$$\lambda(\epsilon_t) = \lambda_1. \tag{4}$$

(b) For noise, noisy chaos, and clean chaos on large scales where memory has lost,

$$\lambda(\epsilon_t) \sim -\gamma \ln \epsilon, \tag{5}$$

where γ is a parameter whose physical meaning will be further discussed below.

(c) For $1/f^{2H+1}$ processes, where $0 < H < 1$ is called the Hurst parameter which characterizes the correlation structure of the process: depending on whether H is smaller than, equal to, or larger than 1/2, the process is said to have anti-persistent, short-range, or persistent long-range correlations [14, 15], we have a diffusive scaling law,

$$\lambda(\epsilon_t) \sim \epsilon^{-1/H}. \tag{6}$$

2.2 Computation of the SDLE

Let $\{V_i, i = 1, 2, \cdots,\}$ be the trajectory in a reconstructed phase space. To compute the SDLE, we first find all the pairs of vectors in the trajectory with their distance approximately ϵ, and then calculate their average distance after a time Δt. The first half of this description amounts to introducing a "shell" (indexed as k),

$$\epsilon_k \le \|V_i - V_j\| \le \epsilon_k + \Delta\epsilon_k, \quad |i-j| > W \tag{7}$$

The parameters ϵ_k (the radius of the shell) and $\Delta\epsilon_k$ (the width of the shell) are arbitrarily chosen small distances. A shell may be considered as a differential element that would facilitate computation of conditional probability. The condition $|i-j| > W$, where W, an integer parameter (which is on the order of the embedding window size $(m-1)L$

for a time series) is used to ensure that the initial separation, $\|V_i - V_j\|$, has aligned with the most unstable direction of the motion [13, 14]. To expedite computation, it is advantageous to introduce a sequence of shells, $k = 1, 2, 3, \cdots$. With all these shells, we can monitor the evolution of all the pairs of vectors (V_i, V_j) within a shell and take average. When each shell is very thin, we have

$$\lambda(\varepsilon_t) = \frac{\left\langle \ln \|V_{i+t+\Delta t} - V_{j+t+\Delta t}\| - \ln \|V_{i+t} - V_{j+t}\| \right\rangle}{\Delta t} \tag{8}$$

where t and Δt are integers in unit of the sampling time, and the angle brackets denote average within a shell. It is clear that

$$\int_0^t \lambda(\varepsilon_t) dt = \left\langle \ln \|V_{i+t} - V_{j+t}\| - \ln \|V_i - V_j\| \right\rangle \tag{9}$$

2.3 Case study

In our previous studies [13, 14], we illustrated the scaling laws described by Eqs. (4) and (5) by the stochastic Lorenz '63 system and other chaotic systems, and the scaling law described by Eq. (6) by the prototypical models for $1/f^{\,2H+1}$ processes, the fractional Brownian motion model and the power-law distributed ON/OFF intermittency. For ease of discussions presented in Sec. 3, we re-illustrate scaling laws described by Eqs. (4) and (5), using the following stochastic Lorenz '63 system:

$$\begin{aligned} dx/dt &= -10(x - y) + D\eta_1(t), \\ dy/dt &= -xz + 28x - y + D\eta_2(t), \\ dz/dt &= xy - \tfrac{8}{3}z + D\eta_3(t), \end{aligned} \tag{10}$$

where $D\eta_i(t),\ i = 1, 2, 3$ are independent Gaussian noise forcing terms with mean 0 and variance D^2. The system is solved using the scheme of Exact propagator [16], where the exact solution of the Lorenz system is solved using a 4-th order Runge-Kutta method with a time-step of $h = 0.002$, and then a term $D\sqrt{h}W$, where W is a Gaussian noise of mean 0 and variance 1, is added to the corresponding equations to take into account the noise. Fig. 1 shows five curves, for the cases of $D = 0, 1, 2, 3, 4$. The computations are done using $m = 4, L = 2$, and 10000 points of the x component of the Lorenz system. For the clean system, we observe two scaling laws. One is Eq. (4), $\lambda(\varepsilon) \approx 0.9$, for small ε, the other is Eq. (5), for large ε where memory has been lost. For the noisy system, the scale region where the scaling law of Eq. (4) shrinks when the stochastic forcing is increased. Interestingly, although the part of the curve with $\lambda(\varepsilon) \sim -\gamma \ln \varepsilon$ shifts to the right when noise is increased, the parameter γ (which is around 1.09 here) appears to not depend on the noise strength.

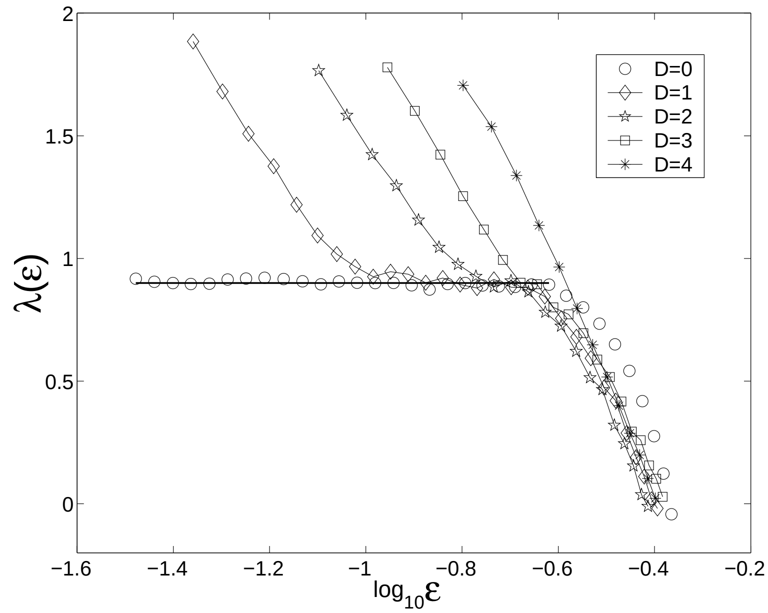

Figure 1: $\lambda(\varepsilon)$ curves for the clean and the noisy Lorenz system.

3 MULTISCALE ANALYSIS OF SEA CLUTTER

3.1 Sea clutter data

Fourteen sea clutter datasets were obtained from a website maintained by Professor Simon Haykin: http://soma.ece.mcmaster.ca/ipix/dartmouth/datasets.html. The measurement was made using the McMaster IPIX radar at Dartmouth, Nova Scotia, Canada. The radar was mounted in a fixed position on land 25-30 m above sea level, with an operating (carrier) frequency of 9.39 GHz (and hence a wavelength of about 3 cm). It was operated at low grazing angles, with the antenna dwelling in a fixed direction, illuminating a patch of ocean surface. The measurements were performed with the wave height in the ocean varying from 0.8 to 3.8 m (with peak heights up to 5.5 m) and the wind conditions varying from still to 60 km/hr (with gusts up to 90 km/hr). For each measurement, 14 areas, called antenna footprints or range bins, were scanned. Their centers are depicted as $B_1, B_2, \cdots, B_{14}$ in Fig. 2. The distance between two adjacent range bins was 15 m. One or a few range bins (say, B_{i-1}, B_i and B_{i+1}) hit a target, which was a spherical block of styrofoam of diameter 1 m wrapped with wire mesh. The locations of the three targets were specified by their azimuthal angle and distance to the radar. They were (128^0, 2660 m), (130^0, 5525 m), and (170^0, 2655 m), respectively. The range bin where the target is strongest is labeled as the primary target bin. Due to drift of the target, bins adjacent to the primary target bin may also have hit the target. They are called secondary target bins. For each range bin, there were 2^{17} complex numbers, sampled with a frequency of 1000 Hz.

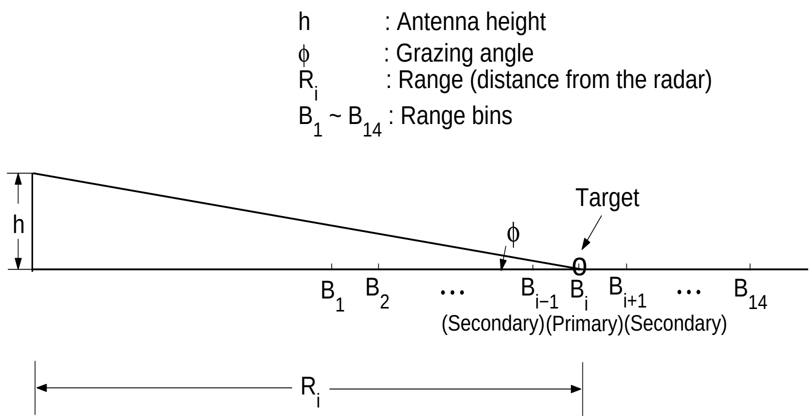

Figure 2: A schematic showing how the sea clutter data were collected.

3.2 Sea clutter analysis

The SDLE curves can be readily computed from sea clutter data. Figure 3(a) shows a typical example. When the γ parameter, which is the slope of the $\lambda(\varepsilon)$ curve, is used to detect targets within sea clutter, we obtain figures like that shown in Fig. 3(b). Clearly, γ is very effective in distinguishing sea clutter with and without targets. For automatic detection purposes, we have analyzed almost 400 datasets available to us and found that a threshold value of 0.9 for γ yields an almost perfect classification:

- Hypothesis H_0: sea clutter without target, $\gamma < 0.9$.
- Hypothesis H_1: sea clutter with target, $\gamma \geq 0.9$.

What is the meaning of γ? To answer this, we consider the concept of the error *doubling time*, defined as the average time for an initial error ε_0 to double: an error grows faster when the doubling time is shorter. In other words, a faster error growth means a more rapid loss of initial information.

What is the error doubling time for sea clutter data? To find this, we use Eq. (3) to get

$$\ln \varepsilon_t = \ln \varepsilon_0 + \int_0^t \lambda(\varepsilon_t) dt. \qquad (11)$$

Letting $\varepsilon_{T_{db}} = 2\varepsilon_0$, we find the error doubling time T_{db} given by

$$\ln 2 = \int_0^{T_{db}} \lambda(\varepsilon_t) dt. \qquad (12)$$

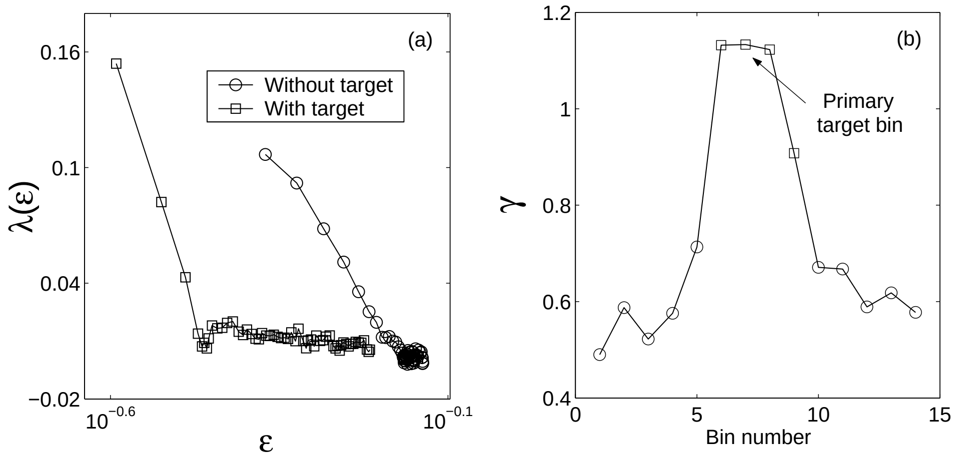

Figure 3: (a) $\lambda(\varepsilon)$ curves for sea clutter. The embedding parameters are $m = 4, L = 1$. (b) Target detection using γ parameter.

As the first approximation, we may consider $1/\lambda(\varepsilon)$ to be proportional to the doubling time. When $\lambda(\varepsilon)$ is given by Eq. (5), then the error doubling time is inversely proportional to γ. Therefore, γ characterizes the speed of information loss. More rigorously, we can prove that $-\ln\varepsilon_0 \gg 1$ decays to a saturation or limiting value of 0 exponentially,

$$-\ln\varepsilon_t = -\ln\varepsilon_0 e^{-\gamma t} \tag{13}$$

A zero magnitude of $\ln\varepsilon_t$ amounts to a unit error. Therefore, it is proper to call γ the relaxation parameter of information loss.

4 CONCLUDING REMARKS

The importance of sea clutter modeling for coastal security, navigation safety, and environmental monitoring has continued to push researchers to better understand the nature of sea clutter. Following Professor Simon Haykin's pioneering work on modeling sea clutter by chaotic dynamics, a number of researchers have examined the chaotic features of sea clutter. Surprisingly, the majority of the works published so far suggests that even though wave-turbulence interactions on the sea surface clearly have their distinct dynamics, sea clutter data are not chaotic when standard chaos theory is used. To resolve once and for all the controversies associated with these exciting researches, and more importantly, to aid in the development of novel methods for detecting small targets within sea clutter, we have employed a newly developed multiscale concept, the SDLE, to study sea clutter. Our analyses of almost 400 sea clutter datasets measured by Professor Simon Haykin suggest that on very short time scales, sea clutter may be classified as noisy chaos, characterized by a parameter γ, which characterizes the speed of information loss. We have further shown that γ can be used to very effectively detect low observable targets within sea clutter.

References

[1] S. Haykin and S. Puthusserypady, "Chaotic dynamics of sea clutter", *Chaos*, **7**, 777-802 (1997).

[2] S. Haykin, *Chaotic dynamics of sea clutter* (John Wiley) 1999.

[3] J.L. Noga, "Bayesian State-Space Modelling of Spatio-Temporal Non-Gaussian Radar Returns", Ph.D thesis, Cambridge University, 1998.

[4] M. Davies, "Looking for Non-Linearities in Sea Clutter", *IEE Radar and Sonar Signal Processing*, Peebles, Scotland, July 1998.

[5] M.R. Cowper and B. Mulgrew, "Nonlinear Processing of High Resolution Radar Sea Clutter", *Proc. IJCNN* **4**, pp. 2633 (1999).

[6] C.P. Unsworth, M.R. Cowper, S. McLaughlin, and B. Mulgrew, "False detection of chaotic behavior in the stochastic compound k-distribution model of radar sea clutter", *Proc. 10th IEEE Workshop on SSAP,* August 2000, pp. 296-300.

[7] C.P. Unsworth, M.R. Cowper, S. McLaughlin, and B. Mulgrew, "Re-examining the nature of sea clutter", *IEE Proc. Radar Sonar Navig.*, **149**, pp. 105-114 (2002).

[8] J.B. Gao and K. Yao, "Multifractal features of sea clutter", *IEEE Radar Conference 2002*, Long Beach, CA, April, 2002.

[9] J.B. Gao, S.K. Hwang, H.F. Chen, Z. Kang, K. Yao, and J.M. Liu, "Can sea clutter and indoor radio propagation be modeled as strange attractors?" *The 7th Experimental Chaos Conference*, San Diego, USA, August pp. 25-29, 2002.

[10] P. Grassberger and I. Procaccia, "Measuring the strangeness of the strange attractor", *Physica D*, **9D**, pp. 189-208 (1983).

[11] S. Haykin, R. Bakker, and B.W. Currie, "Uncovering nonlinear dynamics-the case study of sea clutter", *Proc. IEEE* **90**, 860-881 (2002).

[12] M. McDonald and A. Damini, "Limitations of nonlinear chaotic dynamics in predicting sea clutter returns", *IEE Proc-Radar Son Nav*, vol. 151. pp. 105-113, 2004.

[13] J.B. Gao, J. Hu, W.W. Tung, Y.H. Cao, Distinguishing chaos from noise by scale-dependent Lyapunov exponent. *Phys. Rev. E* **74**, 066204, 2006.

[14] J.B. Gao, Y.H. Cao, W.W. Tung, and J. Hu, *Multiscale Analysis of Complex Time Series — Integration of Chaos and Random Fractal Theory, and Beyond*, Wiley, August, 2007.

[15] J.B. Gao, J. Hu, W.W. Tung, Y.H. Cao, N. Sarshar, V. P. Roychowdhury, Assessment of long range correlation in time series: How to avoid pitfalls. *Phys. Rev. E* **73**, 016117 (2006).

[16] R. Mannella, Integration of stochastic differential equations on a computer. *International J. Modern Phys. C* **13**, 1177-1194, 2002.